




Original Article

Quantifying calibration strategies for capacitive soil-moisture sensors (V1.2 SKU: FA3003-1) in automated drip irrigation for upland, rainfed farms

Carmeli Adele Cabia¹, Ma. Grace C. Sumaria^{1,2*}, Eldon de Padua¹ and Nilo Leorna¹

ABSTRACT

Upland, rainfed farms in the Philippines require precise irrigation to manage scarce water resources efficiently. To address this, we developed an Arduino-based automated drip irrigation system using six low-cost analog capacitive soil-moisture sensors and a normally-closed solenoid valve, triggered by a simple threshold control mechanism. The sensors were calibrated in the laboratory using loamy sand and evaluated through two strategies: a pooled general model and sensor-specific models. Exponential regression yielded the best monotonic fit ($R^2 = 0.94-0.97$). Compared to the general model (RMSE = 2.42–3.37%), sensor-specific calibrations improved both precision (CV < 10%) and accuracy (RMSE = 1.81–2.67%). Although mean differences and R^2 values were not statistically significant (paired T-test, $\alpha = 0.01$), the general equation remains practical for field deployment. However, sensor-specific equations are preferable when higher accuracy is required. At higher moisture levels (36–46% VWC), the sensors tended to overestimate, suggesting increased error near the wet end of the scale. Overall, the low-cost system functioned reliably, demonstrating a viable, moisture-responsive irrigation control solution for small- to medium-sized upland plots.

Keywords: Automation; Regression; Soil Moisture; Soil Moisture Sensor Calibration.

Received: 26 June 2025

Revised: 29 September 2025

Accepted: 10 October 2025

Published: 12 December 2025



©The authors. This is an Open Access article distributed under the terms of the Creative Commons Attribution 4.0 (<https://creativecommons.org/licenses/by-nc-nd/4.0/>)

¹Department of Agricultural and Biosystems Engineering, Visayas State University, Baybay City, Leyte, 6521, Philippines

²Department of Biological and Agricultural Engineering, Faculty of Engineering, Universiti Putra Malaysia, Serdang, Selangor, Malaysia

*Corresponding Author. Address: Department of Agricultural and Biosystems Engineering, Visayas State University, Baybay City, Leyte, 6521, Philippines; Email: grace.sumaria@vsu.edu.ph

INTRODUCTION

Upland farms in the Philippines mostly depend on rainfall and often lack access to consistent and reliable irrigation systems. According to Victoriano (2019), water availability remains a major challenge in these farming areas – a concern also raised in both past and recent studies (Landichoa et al., 2022; Yeleliere et al., 2023). Given these limitations, it is important to use water wisely and efficiently in upland regions where it is scarce.

In response to this need, one promising solution is drip irrigation. As reported by Yang et al. (2023), this system delivers water directly to the plant roots, helping increase crop yields while reducing the use of water, fertilizer, energy, and crop protection products. However, in areas where water sources are limited and flow rates are low, precision in irrigation timing and delivery becomes essential.

To address this challenge more effectively, automating the irrigation process can make a significant difference. Stauffer and Spuhler (2020) explained that automation allows irrigation to start and stop automatically, reducing manual labor and improving scheduling. This is especially helpful in upland systems, where water discharge must be managed carefully, and timing plays a critical role in maximizing efficiency and minimizing waste.

Moreover, soil moisture plays a crucial role in deciding when to irrigate. Ogwo et al. (2020) state that real-time monitoring of soil moisture using sensors provides a more accurate picture of the soil's condition than traditional gravimetric methods. Capacitive sensors, which are affordable and easy to use, make this kind of real-time monitoring possible. However, these sensors do not directly show the actual water content in the soil. To ensure their effectiveness, they need to be calibrated so that their readings can be accurately translated into volumetric water content (VWC) (Placidi et al., 2020; Radi et al., 2018). Additionally, Kinzli et al. (2012) and Kulmány et al. (2022) emphasize that differences in installation – such as cable length or power supply – can cause variations in sensor readings, making individual calibration even more necessary.

In light of these considerations, this study aimed to quantify calibration strategies for capacitive soil-moisture sensors in automated drip irrigation for upland rainfed farms. Specifically, the study compared a general (pooled) calibration model with individual sensor-specific models using different calibration metrics. The ultimate goal was to create a low-cost, accurate, and moisture-based automated irrigation system suited for small to medium-sized upland farms.

MATERIALS AND METHODS

System Design and Components

An automated drip irrigation system was built for small- to medium-sized vegetable plots. It comprised a water tank, distribution pipes, drip lines, and an electronic control assembly for real-time soil-moisture sensing. Figure 1 illustrates the complete layout of the system and its components in a field application.

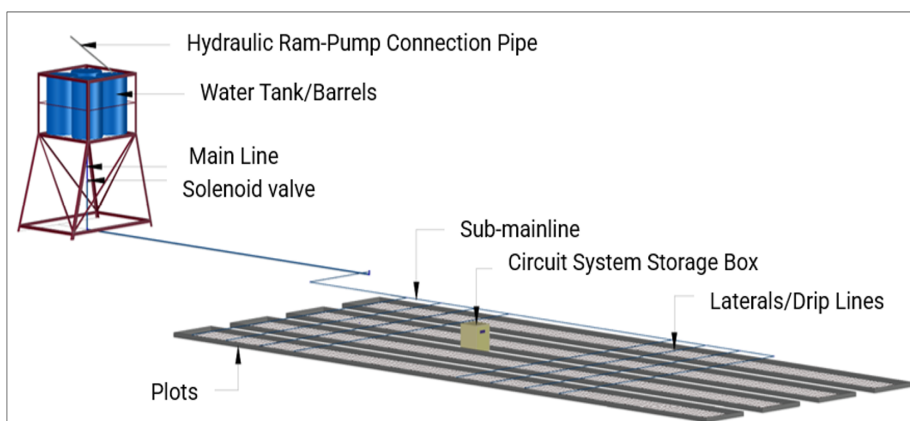


Figure 1. Perspective view of the system in a field application.

Electronic Control Assembly of the System

The electronic control assembly included a control box, soil-moisture sensors, and a solenoid valve (Figures 2-3).

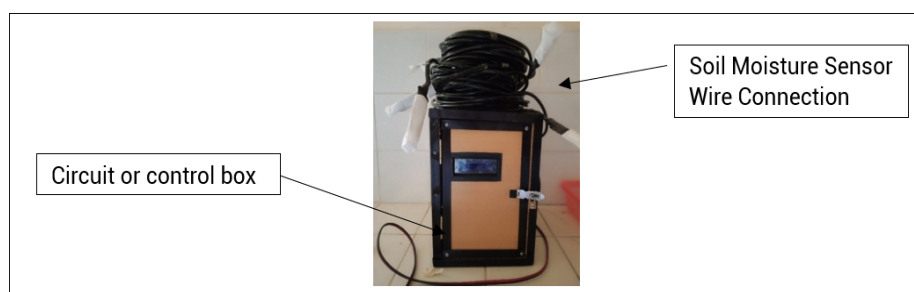


Figure 2. Electronic control assembly.

Control Box

The control box managed sensor inputs, data logging, display, and valve actuation. The core components included the following: (1) Arduino Mega 2560, (2) breadboard, (3) jumper wires, (4) 12 V DC adapter (for the microcontroller and sensors) and 15 V DC adapter (for the solenoid), (5) micro-SD module, (6) DS3231 RTC, (7) 1^oC LCD, (8) 5 V relay module, and (9) a DC power splitter for distributing 12 V to the sensors and controller.

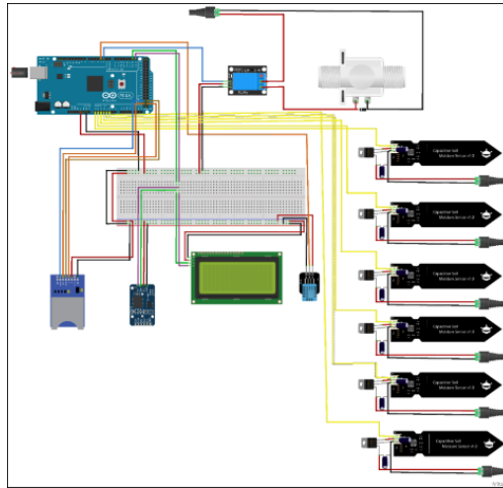


Figure 3. Schematic wiring diagram of the automated drip irrigation system.

Soil Moisture Sensors

As shown in Figure 4, six analog capacitive sensors (V1.2, SKU: FA3003-1) were used (three-pin: analog out, VCC, GND). Because sensors were installed far from the control box, extended leads introduced voltage drop and signal instability. To stabilize supply, each sensor received regulated 5V via an LM7805 with 10 μ F capacitors soldered on the module, powered from a 12V line (Figure 5).



Figure 4. Soil moisture sensors (SKU: FA3003-1)

To mitigate this, 12V external power sources were regulated to 5V using LM7805 voltage regulators soldered onto the sensors, supported by capacitors to ensure a stable power supply (Figure 5).

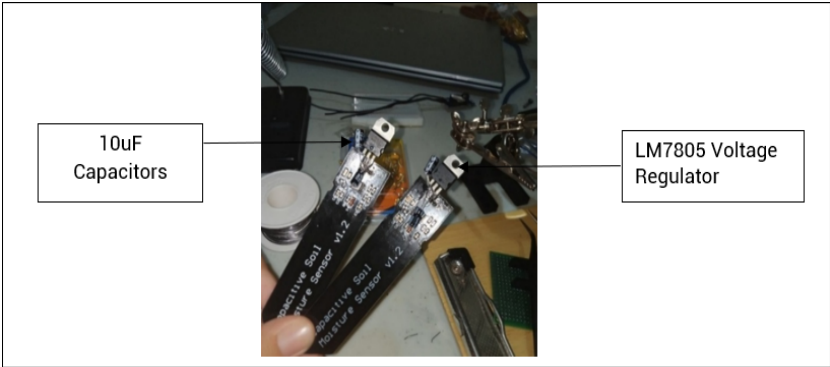


Figure 5. Voltage regulators and capacitors soldered into the sensor module.

Sensor specifications are listed in Table 1. All sensors were installed at 7.5cm depth. This configuration was based on the previous findings of Mane et al. (2021).

Table 1. Specifications of analog capacitive soil moisture sensor V1.2 SKU: FA3003-1

Operating Voltage	3.3 ~ 5.5 VDC
Output Voltage	0 ~ 3.0VDC
Operating Current	5mA
Interface	PH2.0-3P
Dimensions	3.86 x 0.905 inches (L x W)
Weight	15g

Solenoid Valve

A 12 V DC, two-way, normally closed ¾" solenoid valve-controlled flow from the tank to the drip lines (Figure 6). A flyback diode protected the circuit from inductive spikes on shut-off (Figure 7).

A single flyback diode was attached to the solenoid valve circuit to protect the valve from voltage spikes generated when the valve was turned off.



Figure 6. The solenoid valve supplying the system with water.

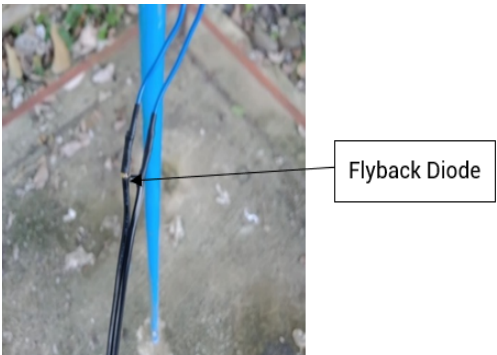


Figure 7. Flyback diode attached to the solenoid valve wiring.

Soil Sample Collection and Preparation

Soil samples were collected from the RERC demonstration farm and tested by the Department of Soil Science - SRTPAL. The soil was classified as loamy sand (4.28% clay, 10% silt, 85.72% sand), with a pH of 6.47 and organic matter content of 2.83%.



Figure 8. Soil samples collected from RERC demo-farm.



Figure 9. Laboratory calibration of soil moisture sensors.

Soil Moisture Calibration

Calibration of soil moisture followed the following procedure:

1. Dried soil was placed in containers large enough for complete sensor submersion. One container was used for each replicate.
2. Ten calibration levels were created by adding increasing amounts of water (increments of 20mL), with three replicates per level.
3. After mixing, each container was weighed (wet weight) and sensor outputs were recorded after a 1min stabilization time.
4. After each level of moisture, the containers were weighed in a digital balance and were recorded as wet weight. This would serve as data to get the gravimetric soil water content of each moisture level. The volume of the container with the corresponding height difference was measured and recorded in each sensor for bulk density measurement (Meter Group, 2022).
5. For confirmation, a soil sample with no added moisture was taken from the containers to oven-dry, ensuring that the soil at the beginning of the calibration was bone-dried or had zero moisture content. Without this condition, the oven-dried soil sample was used as a reference for bone-dry data.

Quantifying calibration strategies for capacitive soil-moisture sensors

Gravimetric Soil Water content can be calculated as follows:

$$MC_{GWC}(\%) = \frac{(M_{wet} - M_{dry})}{(M_{dry})} \times 100 \quad (1)$$

Where:

$MC_{GWC}(\%)$ = Gravimetric soil water content percentage
 M_{wet} = Fresh weight of the soil (g)
 M_{dry} = Dry weight of the soil (g)

Volumetric water content is calculated by multiplying gravimetric water content by the soil bulk density. Bulk density is mass by area of soil.

$$P_b = \frac{M_{dry}}{V_{soil}} \quad (2)$$

Where:

P_b = Soil bulk density (g/cm³)
 M_{dry} = Dry weight of the soil (g)
 V_{soil} = Volume of the soil (cm³)

$$VWC = (MC_{GWC}) \times (P_b) \quad (3)$$

Where:

VWC = Volumetric water content (%)
 P_b = Soil bulk density (g/cm³)

Pre-Calibration, Modelling, and Performance Metrics

Figure 10 presents the implemented data processing and analysis pipeline of the study. Specifically, each of the component processes was carried out as follows:

Sensor Pre-Calibration (Map Scaling). Each sensor underwent dry (in air) and wet (fully submerged) checks to establish lower and upper bounds. Three readings per state were averaged and used to map raw counts to scaled readings in Arduino IDE prior to model fitting.

Calibration Modelling. Sensor-scaled readings (x) were regressed against VWC (y). Two strategies were compared: a general (pooled) model using all sensors' data and sensor-specific models (n = 6) to address variability from differing cable runs (noise/voltage drop). Candidate forms included linear, logarithmic, power, exponential, and 2nd-order polynomial.

Performance metrics. Models were evaluated using Mean, Standard Deviation (SD), Coefficient of Variation (CV), Root-Mean-Square-Error (RMSE), Mean Absolute Error (MAE), and Coefficient of Determination (R²).

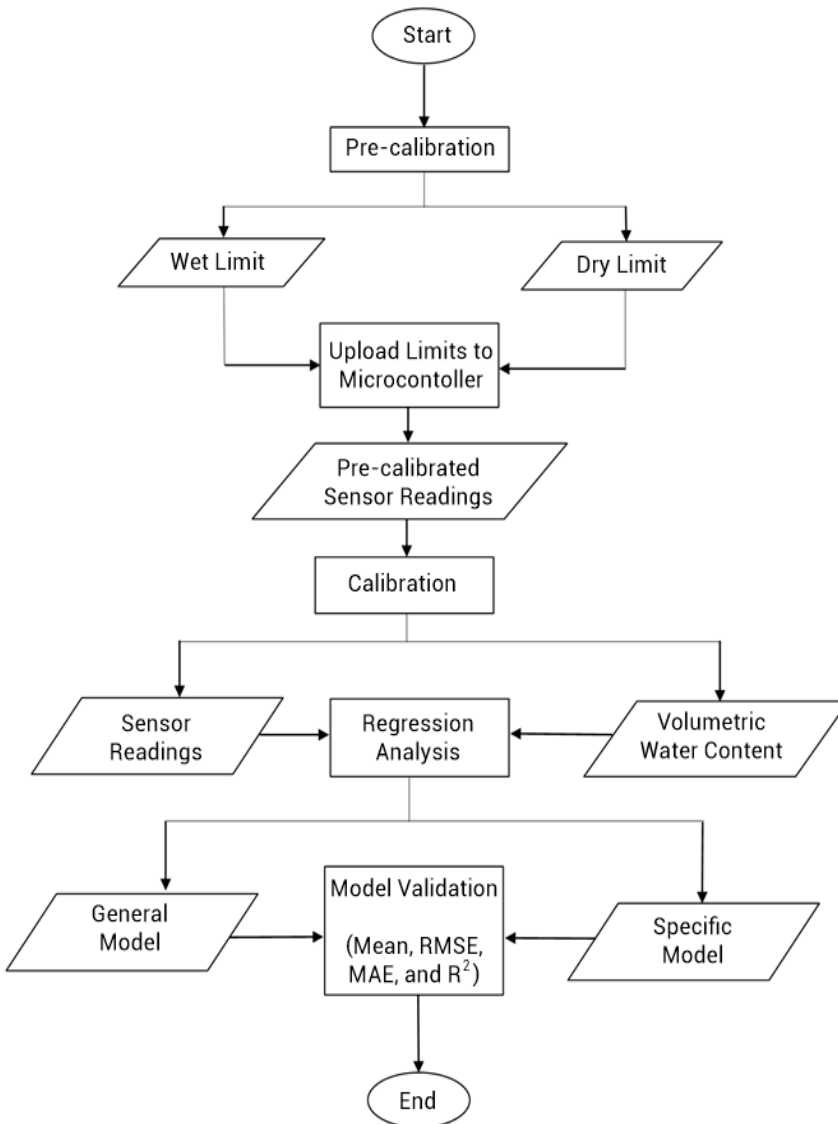


Figure 10. Calibration and modelling process flowchart

RESULTS

An automatic watering controller was integrated into the drip irrigation system using an Arduino Mega 2560, capacitive soil-moisture sensors, and a solenoid valve. The sensors continuously measured soil MC and sent readings to the Arduino. The microcontroller compared each reading with a preset threshold (defined in the IDE). When moisture fell below the threshold, the controller activated the solenoid valve, opening flow from the tank through the sub-main to

the lateral drip lines. While irrigation was underway, the sensors continued to sample the soil. Once moisture rose above the threshold, the controller deactivated the valve, closing it and stopping flow to the sub-main laterals. The system sampled every 3seconds and logged data at 10min intervals.

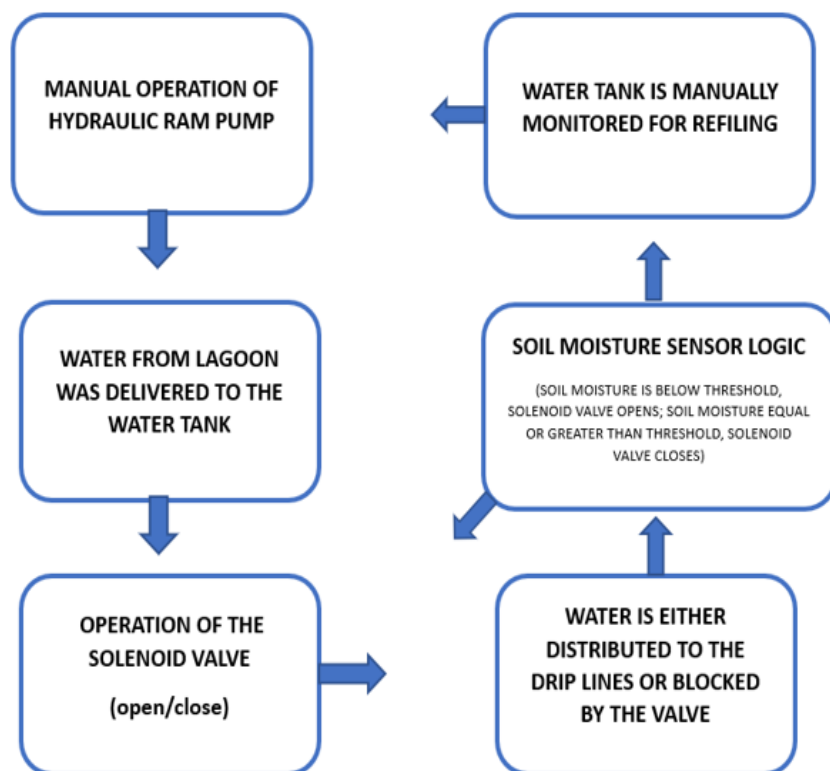


Figure 11. Block diagram of the operational process workflow of the system

Calibration and Modelling

Pre-calibration. System calibration was performed under laboratory conditions. At the start of the process, raw capacitance counts were displayed. Each sensor underwent dry (air) and wet (full-submersion) checks to establish lower and upper bounds (Figure 12). These limits were then used in the Arduino "map()" function to scale raw counts (411-899) to a 0-100% moisture scale. For each moisture increment, the scaled sensor reading, the sample mass, and the change in soil height within the container were recorded.

Modelling. Two calibration approaches were developed:

1. General (pooled) model: a single equation fitted to the combined dataset from all sensors and applied universally.
2. Sensor-specific models: six equations, each fitted to data from its respective sensor.

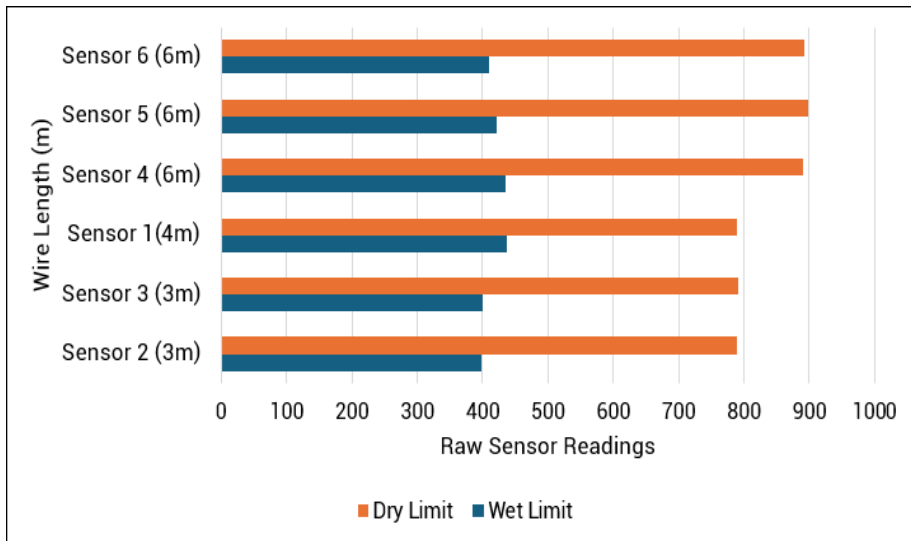


Figure 12. Upper (dry) and lower (wet) limits of the sensors.

Differences among sensors, as shown in Figure 12, and partly due to varying lead lengths, motivated the sensor-specific approach. In all models, x = scaled sensor reading (%) and y = volumetric water content (VWC, %). Regression summaries used for model selection are presented in Table 2.

Table 2. Regression analyses summary of the relationship between volumetric water content and sensor readings.

Sensor No.	Regression Model Type	Regression Model	Coefficient of Determination (R^2)
General	Linear	$y = 0.394x - 2.8855$	0.8422
	Polynomial (2 nd Order)	$y = 0.0045x^2 - 0.1159x + 8.1169$	0.9385
	Exponential	$y = 5.1425e^{0.0204x}$	0.9453
	Power	$y = 1.1519x^{0.6986}$	0.7778
	Logarithmic	$y = 11.968\ln(x) - 25.873$	0.5448
1	Linear	$y = 0.4025x - 0.5406$	0.9341
	Polynomial (2 nd Order)	$y = 0.0029x^2 + 0.0801x + 6.0379$	0.9755
	Exponential	$y = 6.0505e^{0.0201x}$	0.9788
	Power	$y = 1.5107x^{0.6586}$	0.8692
	Logarithmic	$y = 11.519\ln(x) - 22.11$	0.6235
2	Linear	$y = 0.3877x - 1.1909$	0.8959
	Polynomial (2 nd Order)	$y = 0.0033x^2 + 0.0092x + 6.6306$	0.957
	Exponential	$y = 5.7071e^{0.0198x}$	0.963
	Power	$y = 1.5575x^{0.6384}$	0.8175
	Logarithmic	$y = 10.95\ln(x) - 20.753$	0.5785
3	Linear	$y = 0.3941x - 1.9502$	0.888
	Polynomial (2 nd Order)	$y = 0.0037x^2 - 0.0253x + 6.7833$	0.9649
	Exponential	$y = 5.4567e^{0.0203x}$	0.9709
	Power	$y = 1.567x^{0.6326}$	0.7986
	Logarithmic	$y = 10.769\ln(x) - 20.333$	0.5533

Table 2. continued

Sensor No.	Regression Model Type	Regression Model	Coefficient of Determination (R^2)
4	Linear	$y = 0.4183x - 6.3133$	0.8236
	Polynomial (2 nd Order)	$y = 0.0057x^2 - 0.2555x + 9.2387$	0.9634
	Exponential	$y = 4.1572e^{0.0222x}$	0.9641
	Power	$y = 0.557x^{0.8565}$	0.793
	Logarithmic	$y = 14.548\ln(x) - 37.816$	0.551
5	Linear	$y = 0.4291x - 5.9625$	0.8272
	Polynomial (2 nd Order)	$y = 0.0062x^2 - 0.2638x + 9.126$	0.9805
	Exponential	$y = 4.2472e^{0.0228x}$	0.9783
	Power	$y = 0.6879x^{0.8139}$	0.7835
	Logarithmic	$y = 13.77\ln(x) - 34.008$	0.5394
6	Linear	$y = 0.4291x - 5.9625$	0.8272
	Polynomial (2 nd Order)	$y = 0.0056x^2 - 0.2665x + 9.9511$	0.9663
	Exponential	$y = 4.2072e^{0.0216x}$	0.9683
	Power	$y = 0.4567x^{0.9003}$	0.8138
	Logarithmic	$y = 15.417\ln(x) - 41.695$	0.5822

Comparison and Analysis of Corrected Readings for General and Sensor-Specific Models

Table 3 summarizes the mean, standard deviation (SD), and coefficient of variation (CV) of the corrected readings from all six sensors under the general model and their respective sensor-specific models.

Table 3. Mean, standard deviation, and coefficient of variation of corrected readings of all sensors for using the general and specific model.

Observations	Actual VWC (%)	General			Specific		
		(\bar{x})	σ	CV (%)	(\bar{x})	σ	CV (%)
1	5.99	6.07	0.39	6.35	5.85	0.53	9.03
2	10.01	9.91	1.20	12.06	9.67	0.13	1.32
3	11.55	12.70	1.69	13.28	12.51	0.69	5.53
4	13.43	14.24	2.02	14.20	14.06	0.63	4.49
5	16.05	16.55	2.45	14.83	16.44	1.18	7.17
6	19.77	19.20	2.75	14.31	19.16	1.05	5.47
7	22.83	21.56	3.05	14.15	21.61	1.24	5.73
8	26.87	28.80	1.96	6.82	29.22	1.22	4.19
9	36.51	36.94	1.56	4.22	37.85	1.70	4.48
10	46.77	40.50	1.14	2.82	41.67	2.44	5.85

Table 4. Performance metric of the general and specific calibration equations.

Sensor	RMSE (%)		MAE		R ²	
	General	Specific	General	Specific	General	Specific
1	3.37	1.86	2.73	1.50	0.9786	0.9788
2	2.69	1.81	2.05	1.69	0.9632	0.963
3	2.42	2.06	1.68	1.58	0.971	0.9639
4	3.02	2.67	2.51	1.43	0.9587	0.9784
5	2.97	2.21	1.91	1.37	0.9713	0.9784
6	3.08	2.48	2.82	1.42	0.9646	0.9683

The RMSE values of the general equation ranged from 2.42%–3.37%, while those of the specific equations ranged from 1.81%–2.67%.

The general and specific calibration equations also yielded the R² values shown below. Both sets produced coefficients of determination close to 1.0, with only slight differences. Table 5 presents the model performance analysis using the paired t-test method at $p = 0.01$. It is evident that the means and coefficient of determination from both models show no significant differences, while the RMSE and MAE exhibit significant differences between the means.

Table 5. T-test results for performance metrics of general and specific models.

Performance Metric	Mean		P-value
	General	Specific	
Mean	20.65	20.80	0.3535
RMSE*	2.93	2.18	0.0083
MAE*	2.28	1.50	0.0145
R ²	0.97	0.97	0.3405

Note: Metrics with * at the side indicates that there is a statistically significant difference between the means.

Table 6. Specific and general calibration equations generated.

Sensor No.	Calibration Equation	R ²
1	$y = 6.0505e^{0.0201x}$	0.9788
2	$y = 5.7071e^{0.0198x}$	0.963
3	$y = 5.4567e^{0.0203x}$	0.9709
4	$y = 4.1572e^{0.0222x}$	0.9641
5	$y = 4.2472e^{0.0228x}$	0.9783
6	$y = 4.2072e^{0.0216x}$	0.9683
General	$y = 5.1425e^{0.0204x}$	0.9453

Note: Specific calibration equations were used for field application of the automated drip irrigation system.

The figure below summarizes the sensor-calibration results, plotting sensor readings against measured volumetric water content (VWC). The data exhibit a strong exponential relationship, indicating that an exponential model is the most suitable for calibration

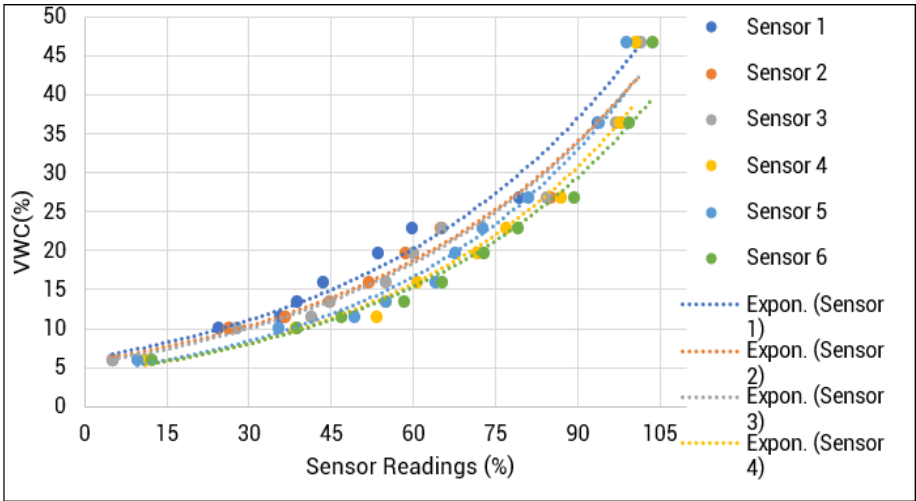


Figure 13. Trendline behavior of initial soil moisture sensor readings against actual VWC.

Figure 14 presents calibrated soil-moisture sensor readings using sensor-specific equations. At observations 9 and 10 (36–46% VWC), most sensors overestimated the actual moisture, resulting in larger errors at higher moisture levels.

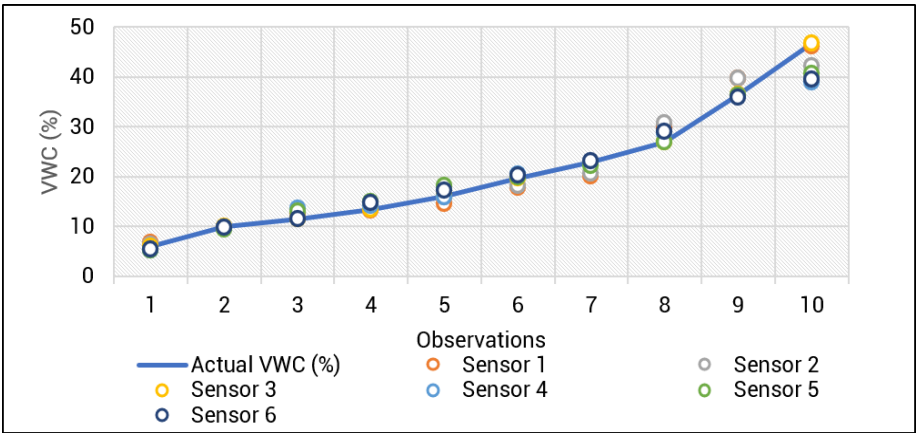


Figure 14. Calibrated soil-moisture sensor readings using sensor-specific equations.

DISCUSSION

For both the general and sensor-specific datasets, linear, exponential, logarithmic, power, and second-order polynomial regressions were fitted. Across all sensors, the logarithmic, power, and linear forms yielded the lowest R^2 values. Although the polynomial fits produced coefficients numerically close to those of the exponential models, their curves were often non-monotonic, rising and falling,

which is unsuitable for control applications, as the system requires a single, consistently increasing response. As shown in Figure 15, higher volumetric water content corresponds to higher scaled sensor readings; therefore, a monotonic model is necessary. Considering both the fit quality and the required response shape, the exponential model was selected for both general and individual calibrations.

In terms of precision, the general model consistently produced higher standard deviations (SDs) across observations compared to the sensor-specific models, indicating lower precision. Specifically, from observations 2 to 7, the coefficients of variation (CVs) under the general model exceeded 10%, reflecting greater dispersion among sensors. In contrast, the CVs from the sensor-specific models remained below 10%. This suggests that the sensor-specific calibrations satisfy the laboratory criterion of $CV \leq 10\%$ for acceptable precision, whereas the general calibration does not.

Regarding accuracy, the RMSE values from the sensor-specific calibration equations align with results from a study that calibrated a soil-moisture capacitance probe in sandy soils, where RMSE values ranged from 1.4% to 2.8% (Campora et al., 2020). By comparison, the RMSE values of the general equation partly fell outside that range.

In addition, across sensors one to six, the mean absolute error (MAE) values from the general model were higher than those from the specific models, indicating that the general model was less accurate. Sensor 6 under the general model recorded the highest MAE, while sensor 5 under the specific model had the lowest. Notably, the MAE values from the specific equations ranged from 1.37 to 1.69, which are considered very good results (Johnson, 1995).

As mentioned in the results, both general and specific equations produced coefficients of determination (R^2) close to 1.0. However, on closer inspection, sensors 1, 4, 5, and 6 showed higher R^2 values under the sensor-specific models. Thus, for the R^2 metric, the decision slightly favors the specific equations. Furthermore, the R^2 values from the specific models align with Campora's findings, which reported R^2 values between 0.96 and 0.99, indicating a strong fit between measurements and calibration equations (Campora et al., 2020). All R^2 values from the sensor-specific equations fall within that range, whereas sensor 4 using the general equation had $R^2 = 0.95$, slightly outside the bounds (Table 4).

Based on these comparisons and analyses, the calibration models recommended for field application are the sensor-specific equations listed in Table 6, due to their higher accuracy and improved inter-sensor consistency. Prior research also reports superior performance of sensor-specific calibrations over general ones (González-Teruel et al., 2019). Nonetheless, for practical purposes and operational efficiency, the general model remains a viable option, as the differences in means and R^2 between the two approaches were not statistically significant.

CONCLUSION

Calibrating analog capacitive soil-moisture sensors individually produced equations with lower MAE and SD and CVs $< 10\%$ (1.32–9.03%), indicating reduced inter-sensor variability (with slight overestimation at higher VWC). These sensor-

specific models also achieved higher R^2 than a single, pooled calibration. Even so, a general equation remains a practical option: in tests (paired T-test, $\alpha = 0.01$), differences in means and R^2 between the two model types were not statistically significant, and a single equation simplifies programming and deployment. Thus, while sensor-specific calibrations are preferred for accuracy, the general calibration is acceptable when simplicity and efficiency are prioritized (lab-based calibration on loamy sand; field recalibration recommended for other soils/conditions). Overall, the automated drip-irrigation system using analog capacitive sensors operated reliably and with good precision.

Acknowledgment

All the authors would like to acknowledge the support from the Renewable Energy Research Center (RERC) and Visayas State University.

Author Contributions

CAC: Conceptualization, data curation, writing-original draft preparation, visualization; MGCS: writing – review and editing, validation & supervision. EPD: writing – review and editing, validation & supervision. NL: validation & supervision. All authors have read and agreed to the published version of the manuscript.

Funding Source

This paper was completed without any external funding or financial support.

Availability of Data and Materials

Data will be made available on request.

Ethical Considerations

Not Applicable.

Competing Interest

The authors declare that they have no competing interests.

References

- Campora, M., Palla, A., Gnecco, I., Bovolenta, R., & Passalacqua, R. (2020). The laboratory calibration of a soil moisture capacitance probe in sandy soils. *Soil and Water Research*, 15(2), 75–84. <https://doi.org/10.17221/227/2018-SWR>
- González-Teruel, J. D., Torres-Sánchez, R., Blaya-Ros, P. J., Toledo-Moreo, A. B., Jiménez-Buendía, M., & Soto-Valles, F. (2019). Design and calibration of a low-cost SDI-12 soil moisture sensor. *Sensors*, 19(3), 491. <https://doi.org/10.3390/s19030491>
- Johnson, D. (1995). *Soil moisture sensor evaluation* (Master's thesis). Tennessee Research and Creative Exchange. https://trace.tennessee.edu/utk_gradthes/6882

- Kinzli, K. D., Manana, N., & Oad, R. (2012). Comparison of laboratory and field calibration of a soil-moisture capacitance probe for various soils. *Journal of Irrigation and Drainage Engineering*, 138(4), 310–321. [https://doi.org/10.1061/\(ASCE\)IR.1943-4774.0000418](https://doi.org/10.1061/(ASCE)IR.1943-4774.0000418)
- Kulmány, I. M., Fazekas, A. B., Beslin, A., Giczi, Z., Milics, G., Kovács, B., Kovács, M., Ambrus, B., Bede, L., & Vona, V. (2022). Calibration of an Arduino-based low-cost capacitive soil moisture sensor for smart agriculture. *Journal of Hydrology and Hydromechanics*, 70(3), 330–340. <https://doi.org/10.2478/johh-2022-0014>
- Landicho, L. D., Cabahuga, R. E. D., Baliton, R. S., & Gonzales, A. B. (2022). Rainwater harvesting for enhancing upland agriculture: Lessons and experiences in selected upland farming communities in Albay Province, Philippines. *APN Science Bulletin*, 12(1), 18–28. <https://doi.org/10.30852/sb.2022.1757>
- METER Group. (2022). *How to calibrate METER soil moisture sensors*. <https://metergroup.com/meter-environment/products/soil-moisture>
- Ogwo, V., Ogbu, K. N., Anyadike, C.C., Nwoke, O. A., & Mbajiorgu, C.C. (2020). Development and testing of a capacitive digital soil moisture sensor with printed circuit board as a probe. *Nigerian Journal of Technology*, 39(3), 911–917. <https://doi.org/10.4314/njt.v39i3.33>
- Placidi, P., Gasperini, L., Grassi, A., Cecconi, M., & Scorzoni, A. (2020). Characterization of low-cost capacitive soil moisture sensors for IoT networks. *Sensors*, 20(12), 3585. <https://doi.org/10.3390/s20123585>
- Radi, M., Murtiningrum, M., Ngadisi, N., Muzdrikah, F. S., Shohibun Nuha, M., & Rizqi, F. A. (2018). Calibration of capacitive soil moisture sensor (SKU: SEN0193). *2018 4th International Conference on Science and Technology (ICST)* (pp. 1–6). <https://doi.org/10.1109/ICSTC.2018.8528624>
- Victoriano, R.A.(2019). *To drip irrigate is to economize*. <https://www.agriculture.com.ph/2019/11/23/to-drip-irrigate-is-to-economize/>
- Stauffer, B., & Spuhler, D. (2020). *Automatic irrigation*. <https://sswm.info/sswm-university-course/module-4-sustainable-water-supply/further-resources-water-use/automatic-irrigation>
- Yang, P., Wu, L., Cheng, M., Fan, J., Li, S., Wang, H., & Qian, L. (2023). Review on drip irrigation: Impact on crop yield, quality, and water productivity in China. *Water*, 15(9), 1733. <https://doi.org/10.3390/w15091733>
- Yeleliere, E., Antwi-Agyei, P., & Guodaar, L. (2023). Farmers' response to climate variability and change in rainfed farming systems: Insight from lived experiences of farmers. *Heliyon*, 9(9), e19656. <https://doi.org/10.1016/j.heliyon.2023.e19656>